

Observation of many-body effects and band-gap renormalization in low-dimensional systems with built-in piezoelectric fields

Karen J. Moore

Department of Mathematics and Physics, The Manchester Metropolitan University, John Dalton Building, Chester Street, Manchester M1 5GD, United Kingdom

Philippe Boring and Bernard Gil

Université de Montpellier II, Groupe d'Etudes des Semiconducteurs, Case Courrier 074, 34095 Montpellier Cedex 5, France

Karl Woodbridge

Department of Electronic and Electrical Engineering, University College London, London WC1E 7JE, United Kingdom

(Received 12 July 1993)

We show that many-body effects and band-gap renormalization can be easily produced in strained-layer quantum wells with internal built-in piezoelectric fields, under photoexcitation. Our observation was made at low temperature by comparing the behavior of $\text{Ga}_{0.92}\text{In}_{0.08}\text{As}$ -GaAs strained-layer quantum wells grown along the (111) and (001) directions and tuning the densities of photoinjected carriers over several decades. Comparison between experimental data and the results of Hartree calculations including the charge space effects reveals that many-body interactions are photoinduced.

Piezoelectricity is a universal property of solids which crystallize in lattices not having inversion symmetry. A recent calculation made for nine zinc-blende-type semiconductors has contributed to the elucidation of the origin of this effect, which has long been under debate.¹ Smith and Mailhot² suggested a few years ago that advantage be taken of such an effect, to produce significant nonlinear optical behavior in some strained-layer semiconductor quantum wells and superlattices. Experimental confirmation of their predictions has now appeared in the literature.³⁻¹⁰

The semiconductor quantum well is simply a thin layer (~ 10 nm) of a small gap semiconductor which, when sandwiched between two layers of higher band-gap compounds acting as barriers, confines the carriers. Strained-layer quantum wells are generally obtained by coherent growth of lattice-mismatched compounds, using modern growth techniques. If growth of strained zinc-blende semiconductors occurs away from the three (001)-like directions, piezoelectric fields are created.¹¹ Straightforward combination of electrostatics with quantum mechanics demonstrates that such a piezoelectric field shifts the wave functions of the conduction and valence bands in opposite ways thus reducing the overlap of the wave functions compared with the zero-field case. Consequently, the optical properties of a quantum well with significant piezoelectric field are *a priori* deteriorated. For a (111)-grown strained-layer quantum well, the radiative lifetime of the interacting electron-hole pair may be larger than for the (001)-grown "equivalent" quantum well.¹¹ This has the advantage of allowing large densities of carriers to be photoinjected into the structures, making them the prototypes for the investigation effects in relation with strong injection of photocarriers. Rather than addressing in this paper an exhaustive list of semiconductor combinations for which piezoelectric fields gave phys-

ical behavior in relation with piezoelectric fields, we select, for instance, Ref. 6. Shanabrook *et al.*⁶ have intensively studied the GaSb-AlSb system, a combination useful for devices working near the $1.55\text{-}\mu\text{m}$ radiation of the optical spectrum. They observed that intersubband energies and interband energies of (111) samples were sensitive to optical-excitation density because the electron-hole pairs screen the piezoelectrically generated electric field. For this combination, the intersubband energies are redshifted under photocarrier injection while the interband energies are blueshifted.

The purpose of this paper is to demonstrate that the onset of band-gap renormalization occurs rapidly under laser illumination. Our results make a significant contribution to the understanding of the physical properties reported so far of semiconductors with built-in piezoelectric fields. The structures we have investigated are strained-layer (Ga,In)As-GaAs single quantum wells grown along the (111) direction by molecular-beam epitaxy. To eliminate the deleterious influence of mobile charges on the piezoelectric effect, we adopted the following designs: starting from an n^+ -type doped ($2 \times 10^{18} \text{ cm}^{-3}$) GaAs substrate, we grew $0.5 \mu\text{m}$ of nonintentionally doped GaAs ($n_a - n_d \sim 10^{15} \text{ cm}^{-3}$), followed by the active part of the sample (here a 10-nm $\text{Ga}_{0.9}\text{In}_{0.10}\text{As}$ layer; nominal values corresponding to fitted values of 9.3 nm and $\text{Ga}_{0.92}\text{In}_{0.08}\text{As}$), $0.5 \mu\text{m}$ of nonintentionally doped GaAs again, and $2\text{-}\mu\text{m}$ beryllium-doped ($p^+ \sim 2 \times 10^{18} \text{ cm}^{-3}$) GaAs. The Fermi level is pinned to the top of the valence and/or conduction band in the p^+ and/or n^+ regions, respectively, giving a $1.5 \times 10^4 \text{ V/cm}$ *nip* field in the undoped region of the samples. Moreover, substrates were chosen to be (111)B-oriented so that the piezoelectric field, which equals some $1.25 \times 10^5 \text{ V/cm}$ in the strained layers, is opposite to the *nip* field. Figure 1 illustrates the differences between the band lineups and first

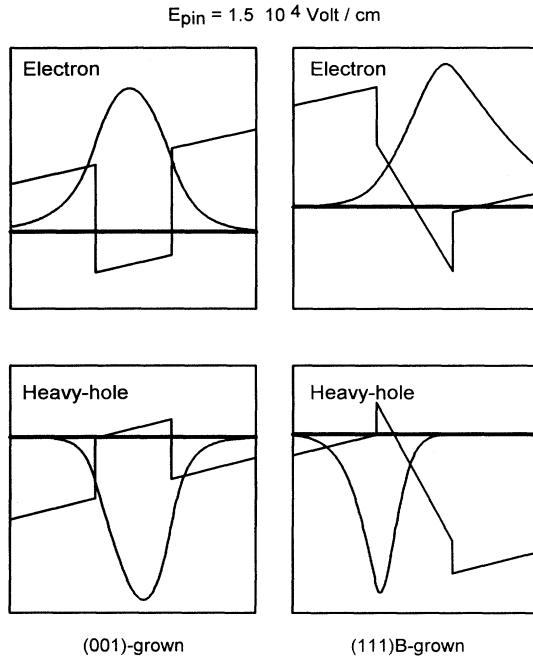


FIG. 1. Schematic of the potential lineups, wave functions, and confined levels for the (001)- and (111)-oriented $\text{Ga}_x\text{In}_{1-x}\text{As-GaAs}$ quantum wells at $\sigma=0$. $\text{Ga}_{0.92}\text{In}_{0.08}\text{As-GaAs}$ strained-layer quantum wells in *pin* diodes. $E_{pin} = 1.5 \times 10^4 \text{ V/cm}$.

conduction, and heavy-hole valence-band envelope functions for the two kinds of samples (001) grown and (111)B grown. Low-temperature (4 K) photoluminescence measurements were made with the samples mounted on the cold finger of a variable-temperature, continuous-flow cryostat. The excitation source was an Ar^+ -pumped Ti-sapphire laser tuned to 810 nm. The excitation density was varied by changing the laser power over more than three orders of magnitude while taking care to ensure that the sample was not heated too much. Figure 2 summarizes the evolution of the photoluminescence spectra as a function of the pump power. As the power is increased, the strength of the signal increases superlinearly. The photoluminescence suddenly broadens when the pump density reaches 200 W/cm^2 , and we note that a weak high-energy shoulder can be observed at 1448 meV. Increasing the pump power, the enlargement of the photoluminescence linewidth increases and this additional structure can no longer be observed. We believe the behavior of the photoluminescence (PL) line shape, in particular its broadening for high excitation conditions is evidence for the existence of a dense electron-hole plasma¹²⁻¹⁶ on the one hand, and sample heating at these pump densities on the other hand. This phenomenon has been intensively studied in conventional GaAs-(GaAl)As heterostructures grown along the (001) direction for which several effects connected to high carrier densities have been observed including (i) the transition from exciton to plasma regime, (ii) band-gap renormalization effects, (iii) Auger scattering mechanisms in the Fermi

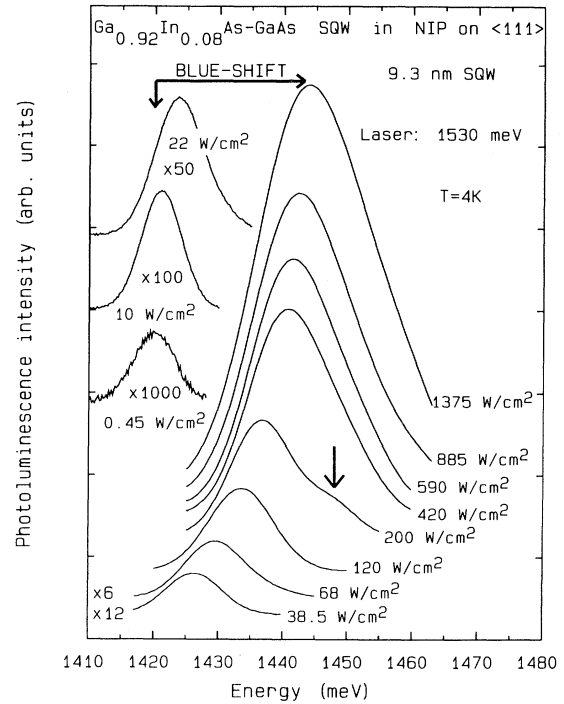


FIG. 2. Pump power dependence of the photoluminescence of the (Ga,In)As-GaAs strained-layer quantum well (111) grown. Note the dramatic blueshift.

sea, (iv) shake-up processes, or (v) hole tunneling.¹²⁻⁴⁴ We note that over our range of excitation densities, we measure a dramatic blueshift of 24 meV of the PL peaks. Moreover, a plot of the PL energies taken from Fig. 2, versus pump power reveals a strong linear slope up to an excitation density of some 120 W/cm^2 , then the slope rapidly bends and saturates as soon as the excitation density reaches 500 W/cm^2 . The experiment was repeated under the same conditions for an identical (001)-grown quantum well, for which the piezoelectric effect does not exist. We did not observe the effects characteristic of the (111) structure. We believe that if the same phenomenon occurs for the two samples, it is dramatically enhanced in the sample where the piezoelectric field coexists and is opposite to the *nip* field.

To explain our observations we must consider a number of phenomenon. First, the effect of space-charge fields caused by the spatial separation of photoinjected electron and holes.²⁶ To calculate the magnitude of the charge space effect, and its implications on the PL with pump power, in the simplest approach, we have to solve self-consistently the equation

$$\left[-\frac{\hbar^2}{2} \frac{\partial}{\partial z} \left[\frac{1}{m_i^*(z)} \right] \frac{\partial}{\partial z} + V(z) + q[F(z) + \Phi(z)]z \right] \chi(z) = E\chi(z) \quad (1)$$

for each type of carrier. In this equation, V is the poten-

tial lineup, F is the total field without injected carriers, and Φ is the contribution of photoinjected electron-hole pairs. In the most general way, at $T \sim 0$ K, Φ is defined as

$$\Phi(z+dz) - \Phi(z) = e\sigma \int_z^{z+dz} \left[\sum_{m,i} \int_0^{k_{\perp}(\sigma)} \alpha_{m,i}(k_{\perp}, \sigma) \chi_{h_{m,i}}^2(k_{\perp}, u) dk_{\perp} - \sum_{n,j} \int_0^{k_{\perp}(\sigma)} \beta_{n,j}(k_{\perp}, \sigma) \chi_{e_{n,j}}^2(k_{\perp}, u) dk_{\perp} \right] \frac{du}{\epsilon(u)}, \quad (2)$$

where the summations are extended over the electron (e) and hole (h) states of interest. Given an areal carrier density σ , one will fill one or several confined subbands up to an appropriate value of the in-plane wave vector k_{\perp} . The indices i and j refer to the lifting of spin degeneracy away from $k_{\perp}=0$, and $\epsilon(z)$ is the dielectric constant. The α and β coefficients are defined such that the additional equations take account of the electric neutrality and concern all the particles trapped in the well:

$$\int_{-\infty}^{+\infty} \left[\sum_{m,i} \int_0^{k_{\perp}(\sigma)} \alpha_{m,i}(k_{\perp}, \sigma) \chi_{h_{m,i}}^2(k_{\perp}, u) dk_{\perp} \right] du = 1, \quad (3a)$$

$$\int_{-\infty}^{+\infty} \left[\sum_{n,j} \int_0^{k_{\perp}(\sigma)} \beta_{n,j}(k_{\perp}, \sigma) \chi_{e_{n,j}}^2(k_{\perp}, u) dk_{\perp} \right] du = 1. \quad (3b)$$

At a given σ , the α or/and β coefficients equal zero for empty states. In our experiment it is possible that several subbands may be populated, due to the range of values of σ ($\sim 10^{12}$ cm $^{-2}$). In order to connect the filling energy E_f of the fundamental subbands to σ through a Fermi vector k_f , we have adopted a simple parabolic model for both conduction and valence states. Figure 3 displays the energy differences between the valence subbands at $k_{\perp}=0$, as a function of σ . We note that the Fermi energy

exceeds the hh_2 - hh_1 energy difference as soon as σ is larger than $\sim 6 \times 10^{11}$ cm $^{-2}$. At this point we have a hole Fermi sea for which two subbands having identical densities of states are occupied. We note that the proximity of the first light-hole state may introduce some nonparabolicity. Concerning the electrons, the e_1 - e_2 splitting equals some 40 meV, it weakly increases with σ , and one only populates the lowest state when $\sigma < 1.5 \times 10^{12}$ cm $^{-2}$.

Typical wave functions resulting from our self-consistent calculation are given in Fig. 4, shown here for two areal electron-hole plasma densities. At $\sigma = 10^{11}$ cm $^{-2}$ [Fig. 4(a)], although we calculate a blueshift with respect to $\sigma=0$, the built-in piezoelectric field is so strong that neither the wave function nor the potential lineups (see inset) have been significantly altered on the scale of the picture. The calculation of $\sigma = 3 \times 10^{12}$ cm $^{-2}$ [Fig. 4(b)] illustrates both the modification of the wave functions and the strong nonlinearities of the potential lineups. Figure 5 summarizes the essential results of the calculation. Figure 5(c) shows the change of the overlap integrals between the first electron and three hole states. Clearly, except for e_1 hh_1 , there is no straightforward relationship with the average electron-hole separations shown in Fig. 5(b). A plot of the transition energies as a function of σ is shown in Fig. 5(a) where the area of the circles is proportional to the band-to-band oscillator strengths. In light of all the information displayed in Fig. 5, we are able to attribute the 1448-meV shoulder (see

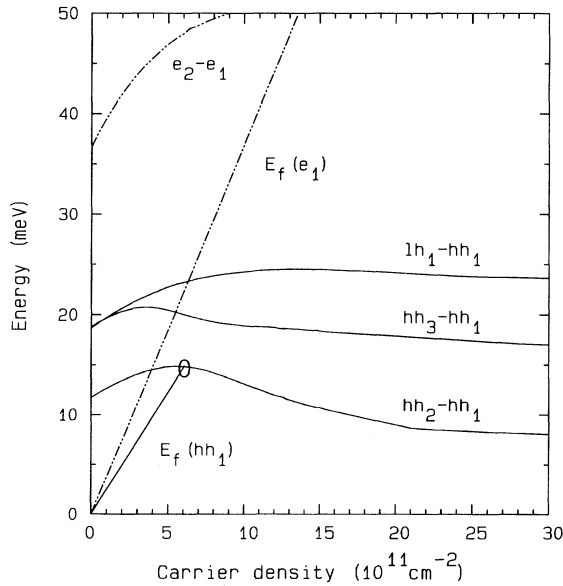


FIG. 3. Energy separations between valence and conduction subbands as a function of the areal carrier density. The Fermi energies are also plotted. Carrier density (a) 30×10^{11} cm $^{-2}$; (b) 1×10^{11} cm $^{-2}$.

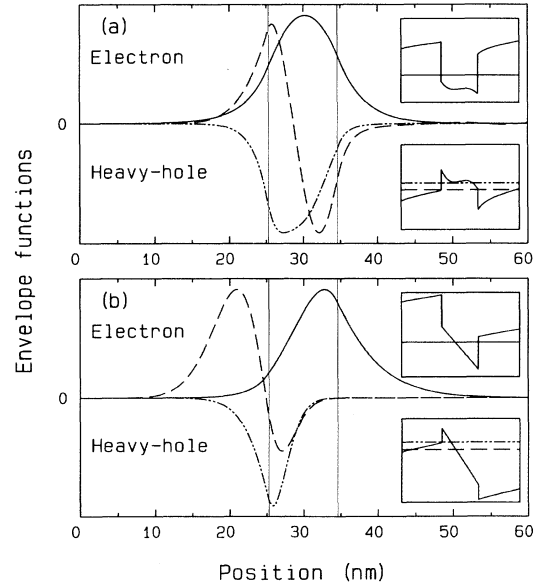


FIG. 4. Plot of self-consistent wave functions for the first electron and two heavy-hole confined states. The potential lineups and positions of the confined states are inserted. The data are given for two areal carrier concentrations.

vertical arrow in Fig. 2) that is resolved under 200 W/cm² excitation to PL from e_1hh_2 made possible to observe when the hole Fermi energy crosses the second heavy-hole band. Then we make this linear relationship between the pump density and the areal photocarrier density: 200 W/cm² $\sim 6 \times 10^{11}$ cm⁻². This corresponds with density-independent radiative lifetimes of some ns. The density dependence of the lifetime has been recently measured (second paper of Ref. 16) for GaAs-(Ga,Al)As. Extrapolation of these data to our sample shows that, in our case, it slightly decreases with carrier density. In our experiment a factor of 2–3 is expected between 10^{11} and 10^{12} cm⁻². This will not have significant implications on the deduction of band-gap renormalization given in Fig. 6.

Comparison between our calculation and experimental observations reveals a significant discrepancy. We calculate a blueshift that is twice the measured value. This difference is attributed to the generation of band-gap renormalization processes by photocarriers. An exact theoretical description for such samples is not within the scope of this paper. This phenomenon has been intensively studied in (001)-grown quantum wells, but its observation has not yet been reported in quantum wells having built-in piezoelectric fields. The interest in these samples is that we could continuously tune the carrier concentrations using rather moderate laser intensities. Our results demonstrate the clear fact that, even in the

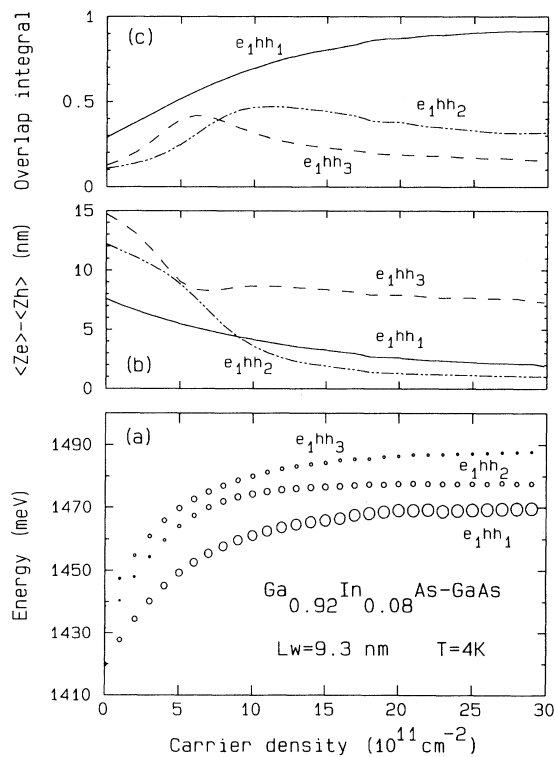


FIG. 5. Plot of typical data obtained from the self-consistent calculation including: (a) transition energies, (b) average electron-hole distance, and (c) overlap integral for the sample with piezoelectric field. See text for details.

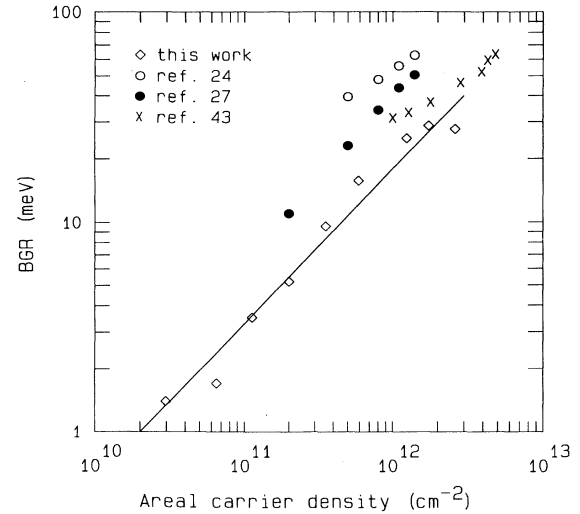


FIG. 6. Band-gap renormalization deduced from our work (open diamonds) and from two theoretical examinations (open, full circles, and crosses for Refs. 24, 27, and 43, respectively).

absence of piezoelectric field which almost cancels the excitonic interaction, for the range of carrier densities we created, the simple picture of the excitonic approach of the electron-hole interaction no longer remains appropriate. Indeed, as it was previously discussed by Schmitt-Rink, Chemla, and Miller¹⁹ who have proposed a heuristic description of the many-body phenomena in pure two-dimensional systems, when the average distance between the photocreated carriers reaches about twice the (2D) Bohr diameter, a transition is expected to occur between this *classical* regime of two interacting particles and an interacting regime more complex involving many-body effects. Under these conditions, a theoretical calculation which self-consistently accounts for all many-body effects is required. This has been addressed via calculations having time-increasing degrees of sophistication.^{16–27,43} Due to the aforementioned difficulties to treat exactly the theoretical problem, and in line with approximations usually made in the literature, we estimate the carrier concentration dependence of the band-gap renormalization by subtracting the experimental energy from the value calculated without including the many-body effects.³² This is shown in Fig. 6. Because the basic principles of the theory are generally expressed as power laws of the carrier concentration, our data are plotted logarithmically (squares). We also include recently reported results of calculations (open, full circles, and crosses for Refs. 24, 27, and 43, respectively). We note that the most recent calculation of Ryan and Reinecke⁴³ gives a good account of the trends observed in our experiment, and that we find a slope larger than the values $\frac{1}{3}$ and $\frac{1}{2}$ predicted by elementary (if already sophisticated) theories for the pure 3D and 2D situations.⁴⁵ The calculations of Refs. 24 and 27 give the slope, but higher renormalization values. The reasons we invoke here to explain qualitatively this discrepancy are first, the influence of the piezoelectric field and second, the difference between

sample designs and the mechanisms which produce the renormalization (photocreated electron-hole pairs in our work and in Ref. 43).

To conclude, we wish to emphasize the fact that non-linear optical properties can easily be induced by photoexcitation in discrete heterostructures having large internal built-in piezoelectric fields. Many-body effects can appear rapidly under laser illumination; this makes such a system very interesting for fundamental physics since the charge densities are easily tuned over several decades. Moreover, in such structures the internal field can be more than one order of magnitude stronger than the

field one induces in biased devices, offering the potential for advanced self-optic or electro-optic devices. The understanding of this physics undoubtedly requires progress in the description of the many-body effects, which had probably not been as readily observed, for this class of artificial semiconductors.

ACKNOWLEDGMENTS

We thank G. Bastard, G. Duggan, R. Resta, J. J. Davies, and C. Mailhot for discussions. The "Groupe d'Etudes des Semiconducteurs is Laboratoire Associé au CNRS."

- ¹Stefano di Geroncoli, Stefano Baroni, and Raffaele Resta, *Phys. Rev. Lett.* **62**, 2853 (1989); *Ferroelectrics* **111**, 19 (1990), and references therein; Andrea Dal Corso, Raffaele Resta, and Stefano Baroni, *Phys. Rev. B* **47**, 16 252 (1993).
- ²D. L. Smith and C. Mailhot, *Rev. Mod. Phys.* **62**, 173 (1990); *Crit. Rev. Solid State Mater. Sci.* **16**, 131 (1990).
- ³B. Laurich, K. Elcess, C. G. Fonstad, J. G. Beery, C. Mailhot, and D. L. Smith, *Phys. Rev. Lett.* **62**, 649 (1989).
- ⁴E. A. Caridi, T. Y. Chang, K. W. Goosen, and L. F. Eastman, *Appl. Phys. Lett.* **56**, 659 (1990); K. W. Goosen, E. A. Caridi, T. Y. Chang, J. B. Stark, D. A. B. Miller, and R. A. Morgan, *ibid.* **56**, 715 (1990).
- ⁵B. K. Laurich, D. L. Smith, D. E. Watkins, I. Sela, S. Subanna, and H. Kroemer, *Superlatt. Microstruct.* **9**, 499 (1991); I. Sela, D. E. Watkins, B. K. Laurich, D. L. Smith, S. Subanna, and H. Kroemer, *Appl. Phys. Lett.* **58**, 684 (1991).
- ⁶B. V. Shanabrook, D. Gammon, R. Beresford, W. I. Wang, R. P. Leavitt, and D. A. Broido, *The Physics of Semiconductors*, edited by E. M. Anastassakis and J. D. Joannopoulos (World Scientific, Singapore, 1990), p. 901; B. V. Shanabrook, D. Gammon, R. Beresford, W. I. Wang, R. P. Leavitt, and D. A. Broido, *Superlatt. Microstruct.* **7**, 363 (1990); G. Brozak, B. V. Shanabrook, D. Gammon, D. A. Broido, R. Beresford, and W. I. Wang, *Surf. Sci.* **267**, 120 (1992).
- ⁷R. André, C. Deshayes, J. Cibert, Le Si Dang, S. Tatarenko, and K. Saminadayar, *Phys. Rev. B* **42**, 11 392 (1990); J. Cibert, R. André, C. Deshayes, Le Si Dang, H. Okumura, S. Tatarenko, G. Feuillet, P. H. Jouneau, R. Mallard, and K. Saminadayar, *J. Cryst. Growth* **117**, 424 (1992).
- ⁸M. P. Halsall, J. E. Nicholls, J. J. Davies, B. Cockayne, and P. J. Wright, *J. Appl. Phys.* **71**, 907 (1992), and references therein.
- ⁹T. S. Moise, L. J. Guido, J. C. Beggy, T. J. Cunningham, S. Seshadri, and R. C. Barker, *J. Electron. Mater.* **21**, 119 (1992); T. S. Moise, L. J. Guido, R. C. Barker, J. O. White, and A. R. Kost, *Appl. Phys. Lett.* **60**, 2637 (1992); T. S. Moise, L. J. Guido, and R. C. Barker, *Phys. Rev. B* **47**, 6758 (1993).
- ¹⁰M. Lakrimi, R. W. Martin, C. Lopez, D. M. Symons, E. T. R. Chidley, R. J. Nicholas, N. J. Mason, and P. J. Walker, *Semicond. Sci. Technol.* **8**, 367 (1993).
- ¹¹P. Bigenwald, B. Gil, and P. Boring, *Phys. Rev. B* **48**, 9122 (1993).
- ¹²M. S. Skolnick, J. M. Rorison, K. J. Nash, D. J. Mowbray, P. R. Tapster, S. J. Bass, and A. D. Pitt, *Phys. Rev. Lett.* **58**, 2130 (1987).
- ¹³G. Trankle, E. Lach, A. Forchel, F. Scholz, C. Hell, H. Haug, G. Weimann, G. Griffiths, H. Kroemer, and S. Subanna, *Phys. Rev. B* **36**, 6712 (1987).
- ¹⁴H. Yoshimura, G. E. W. Bauer, and H. Sakaki, *Phys. Rev. B* **38**, 10 791 (1987).
- ¹⁵C. Colvard, N. Nouri, H. Lee, and D. Ackley, *Phys. Rev. B* **39**, 8033 (1989).
- ¹⁶G. Bongiovanni and J. L. Staehli, *Phys. Rev. B* **39**, 8359 (1989); **46**, 9861 (1992).
- ¹⁷G. E. W. Bauer and T. Ando, *Phys. Rev. B* **31**, 8321 (1985); *J. Phys. C* **19**, 1537 (1986); *Phys. Rev. B* **34**, 1300 (1986).
- ¹⁸D. A. Kleiman and R. C. Miller, *Phys. Rev. B* **32**, 2266 (1985).
- ¹⁹S. Schmitt-Rink, D. S. Chemla, and D. A. B. Miller, *Phys. Rev. B* **32**, 6601 (1985).
- ²⁰S. Schmitt-Rink, C. Hell, and H. Haug, *Phys. Rev. B* **33**, 1183 (1986).
- ²¹D. A. Kleiman, *Phys. Rev. B* **33**, 2540 (1986).
- ²²A. E. Ruckenstein, S. Schmitt-Rink, and R. C. Miller, *Phys. Rev. Lett.* **56**, 504 (1986).
- ²³A. E. Ruckenstein and S. Schmitt-Rink, *Phys. Rev. B* **35**, 7551 (1987).
- ²⁴S. das Sarma, R. Jalabert, and S. R. Eric-Yang, *Phys. Rev. B* **41**, 8288 (1990).
- ²⁵E. X. Ping and H. X. Jiang, *Phys. Rev. B* **47**, 2101 (1993).
- ²⁶R. Binder, I. Galbraith, and S. W. Koch, *Phys. Rev. B* **44**, 3301 (1991).
- ²⁷P. Von Allmen, *Phys. Rev. B* **46**, 13 345 (1992).
- ²⁸N. Peyghambarian, H. M. Gibbs, J. L. Jewell, A. Antonetti, A. Migus, D. Hulin, and A. Mysyrowicz, *Phys. Rev. Lett.* **53**, 2433 (1984).
- ²⁹D. Hulin, A. Mysyrowicz, A. Antonetti, A. Migus, W. T. Masselink, H. Morkoç, H. M. Gibbs, and N. Peyghambarian, *Phys. Rev. B* **33**, 4389 (1986).
- ³⁰T. Uenoyama and L. J. Sham, *Phys. Rev. Lett.* **65**, 1048 (1990).
- ³¹R. Sooryakumar, A. Pinckzuk, A. C. Gossard, D. S. Chemla, and L. J. Sham, *Phys. Rev. Lett.* **58**, 1150 (1987).
- ³²C. Delalande, G. Bastard, J. Orgonasi, J. A. Brum, H. W. Liu, M. Voos, G. Weimann, and W. Schlapp, *Phys. Rev. Lett.* **59**, 2690 (1987).
- ³³C. Weber, C. Klingshirn, D. S. Chemla, D. A. B. Miller, J. E. Cunningham, and C. Hell, *Phys. Rev. B* **38**, 12 748 (1987).
- ³⁴H. Kalt, K. Leo, R. Cingolani, and K. Ploog, *Phys. Rev. B* **40**, 12 017 (1989).
- ³⁵K. H. Schlaad, C. Weber, J. Cunningham, C. V. Hoof, G. Borghs, G. Weimann, W. Schlapp, H. Nickel, and C. Klingshirn, *Phys. Rev. B* **43**, 4268 (1989).

- ³⁶M. S. Skolnick, D. M. Whittaker, P. E. Simmonds, T. A. Fisher, M. K. Saker, J. M. Rorison, R. S. Smith, P. B. Kirby, and C. R. H. White, *Phys. Rev. B* **43**, 7354 (1991).
- ³⁷M. Potemski, R. Stepniewski, J. C. Maan, G. Martinez, P. Wyder, and B. Etienne, *Phys. Rev. Lett.* **66**, 2239 (1991).
- ³⁸G. R. Olbright, W. S. Fu, A. Owyong, J. F. Klem, R. Binder, I. Galbraith, and S. W. Koch, *Phys. Rev. Lett.* **66**, 1358 (1991); G. R. Olbright, W. S. Fu, J. F. Klem, H. M. Gibbs, G. Khitrova, R. Pon, B. Fluegel, K. Meissner, N. Peyghambarian, R. Binder, I. Galbraith, and S. W. Koch, *Phys. Rev. B* **44**, 3043 (1991).
- ³⁹I. Galbraith, P. Dawson, and C. T. Foxon, *Phys. Rev. B* **45**, 13 499 (1992).
- ⁴⁰P. E. Simmonds, M. S. Skolnick, T. A. Fischer, K. J. Nash, and R. S. Smith, *Phys. Rev. B* **45**, 9497 (1992).
- ⁴¹Y. F. Chen, L. Y. Lin, L. J. Shen, and D. W. Liu, *Phys. Rev. B* **46**, 8359 (1992).
- ⁴²E. Lach, A. Forchel, D. A. Broido, T. L. Reinecke, G. Weimann, and W. Schlapp, *Phys. Rev. B* **42**, 5395 (1990).
- ⁴³J. C. Ryan and T. L. Reinecke, *Phys. Rev. B* **47**, 9613 (1993).
- ⁴⁴B. Boring, B. Gil, and K. J. Moore, *Phys. Rev. Lett.* **71**, 1875 (1993).
- ⁴⁵H. Haug and S. W. Koch, *Quantum Theory and Optical Properties of Semiconductors* (World Scientific, Singapore, 1990).